ELSEVIER

Ceramics International 30 (2004) 1009–1016

CERAMICS INTERNATIONAL

www.elsevier.com/locate/ceramint

Electrical properties and DC-accelerated aging behavior of ZnO–Pr_6O_{11}–CoO–Cr_2O_3–Dy_2O_3-based varistor ceramics

Choon-Woo Nahm [a,*], Jong-Ah Park [a], Byoung-Chul Shin [b], Il-Soo Kim [b]

[a] *Department of Electrical Engineering, Dongeui University, Busan 614-714, South Korea*
[b] *Department of Information Materials Engineering, Dongeui University, Busan 614-714, South Korea*

Received 26 May 2003; received in revised form 26 September 2003; accepted 14 October 2003

Available online 19 March 2004

Abstract

The microstructure, electrical properties, and DC-accelerated aging behavior of varistor ceramics, which are composed of ZnO–Pr_6O_{11}–CoO–Cr_2O_3–Dy_2O_3 (ZPCCD)-based ceramics, were investigated in the range of 0.0–2.0 mol% Dy_2O_3. As Dy_2O_3 content is increased, the density was decreased in the range of 5.53–4.43 g/cm^3 and the average ZnO grain size was decreased in the range of 18.6–4.7 μm. The varistors with Dy_2O_3 exhibited a high nonlinear exponent above 30, compared with that without Dy_2O_3. The incorporation of Dy_2O_3 significantly improved the nonlinear properties of ZPCCD-based varistors. The varistor with Dy_2O_3 content of 0.5 mol% exhibited the highest nonlinearity, in which a nonlinear exponent is 66.6 and a leakage current is 1.2 μA. Furthermore, this varistor showed the high stability, in which the variation rate of varistor voltage, of nonlinear exponent, and of leakage are −1.9, −10.5, and +288.8%, respectively, under DC-accelerated aging stress, 0.95 V_{1mA}/150 °C/24 h, respectively, with increasing Dy_2O_3 content.

Keywords: B. Microstructure; C. Electrical properties; E. Varistors; Pr_6O_{11}; Dy_2O_3; ZPCCD-based varistors

1. Introduction

Zinc oxide (ZnO) varistors are smart electronic ceramic devices made by sintering ZnO powder with minor metal oxides containing necessarily Pr_6O_{11} or Bi_2O_3, providing individual roles. They exhibit highly nonlinear voltage–current (V–I) characteristics expressed by $I = kV^{\alpha}$, where k is a constant and α is a nonlinear exponent, inherent parameter of varistors, that is, they act as an insulator due to high impedance below critical voltage and as a conductor due to extremely low impedance above critical voltage. And they possess excellent surge withstanding capabilities. Therefore, they have been widely used to protect semiconductor devices, electronic circuits, and electric power systems from dangerous overvoltage [1,2].

The majority of commercial ZnO varistors necessarily contain Bi_2O_3 as varistor-forming oxides (VFO) and they exhibit excellent varistor properties. However, they have a few drawbacks due to the high volatility and reactivity of Bi_2O_3 melted at about 825 °C during a sintering above 1000 °C [3]. The former changes varistor characteristics with the variation of inter-composition ratio of additives, the latter destroys the multi-layer structure of chip varistors and it generates many secondary phases in addition to insulating spinel phase deteriorating surge-absorption capabilities.

In the past few years, it has been studying ZnO varistor ceramics containing Pr_6O_{11} as VFO to overcome these problems [4–21]. In the former work, Nahm et al. reported that ZnO–Pr_6O_{11}–CoO–Cr_2O_3–M_2O_3 (M = Er, Y)-based varistor ceramics exhibit high nonlinear properties and stability [12–21]. Many researchers who are interested in varistors wish to fabricate ZnO varistors exhibiting both higher nonlinearity and higher stability. It is very important to scrutinize the role of individual additive to apply ZnO–Pr_6O_{11}-based varistors in various areas.

The purpose of this work is to investigate the effect of Dy_2O_3 incorporation on microstructure, electrical properties, and DC-accelerated aging behavior of ZnO–Pr_6O_{11}–CoO–Cr_2O_3–Dy_2O_3 (in short ZPCCD)-based varistors.

* Corresponding author. Tel.: +82-51-890-1669; fax: +82-51-890-1664.
E-mail address: cwnahm@dongeui.ac.kr (C.-W. Nahm).

0272-8842/$30.00 © 2004 Elsevier Ltd and Techna Group S.r.l. All rights reserved.
doi:10.1016/j.ceramint.2003.10.020

2. Experimental procedure

2.1. Sample preparation

Reagent-grade raw materials were prepared for ZnO varistors with composition $(98.0 - x)$ mol% ZnO + 0.5 mol% Pr_6O_{11} + 1.0 mol% CoO + 0.5 mol% Cr_2O_3 + x mol% Dy_2O_3 (x = 0.0, 0.5, 1.0, 2.0). The chemicals were weighed and ball-milled with ZrO_2 balls and acetone in a polypropylene bottle for 24 h. The mixture was dried at 120 °C for 12 h and calcined at 750 °C for 2 h. The calcined mixture was pulverized using an agate mortar/pestle and after 2 wt.% polyvinyl alcohol (PVA) binder addition, granulated by sieving 200-mesh screen to produce starting powder. The powders were uniaxially pressed into discs of 10 mm in diameter and 1.8 mm in thickness at a pressure of 80 MPa. The discs were sintered at 1350 °C in air for 1 h. The size of the final samples was about 8 mm in diameter and 1.0 mm in thickness. Silver paste was coated on both faces of the samples and ohmic contacts were formed by heating at 600 °C for 10 min. The electrodes were 5 mm in diameter.

2.2. Microstructure measurement

The either surface of samples was lapped and ground with SiC paper and polished with 0.3 μm-Al_2O_3 powder to a mirror-like surface. The polished samples were thermally etched at 1100 °C for 30 min. The surface microstructure was examined by a scanning electron microscope (SEM, Hitachi S2400, Japan). The average grain size (d) was determined by the lineal intercept method, given by $d = 1.56L/MN$, where L is the random line length on the micrograph, M is the magnification of the micrograph, and N is the number of the grain boundaries intercepted by lines [22]. The crystalline phases were identified by an X-ray diffractometry (XRD, Rigaku D/max 2100, Japan) with Cu Kα radiation. The density (ρ) of varistor ceramics was measured by the Archimedes method.

2.3. Electrical measurement

The voltage–current (V–I) characteristics of the varistors were measured using a high voltage source-measure unit (Keithley 237). The varistor voltage ($V_{1\,mA}$) was measured at a current density of 1.0 mA/cm^2 and the leakage current (I_L) was measured at 0.80 $V_{1\,mA}$. In addition, the nonlinear exponent (α) was determined from $\alpha = (\log J_2 - \log J_1)/(\log E_2 - \log E_1)$, where J_1 = 1.0 mA/cm^2, J_2 = 10 mA/cm^2, and E_1 and E_2 are the electric fields corresponding to J_1 and J_2, respectively.

The capacitance–voltage (C–V) characteristics of varistors were measured at 1 kHz using a RLC meter (QuadTech 7600) and an electrometer (Keithley 617). The donor concentration (N_d) and the barrier height (ϕ_b) were determined by the equation $(1/C_b - 1/C_{bo})^2 = 2(\phi_b + V_{gb})/q\varepsilon N_d$ [23], where C_b is the capacitance per unit area of a grain boundary, C_{bo} is the value of C_b when $V_{gb} = 0$, V_{gb} is the applied voltage per grain boundary, q is the electronic charge, ε is the permittivity of ZnO ($\varepsilon = 8.5\varepsilon_o$). The density of interface states (N_t) at the grain boundary was determined by the equation $N_t = (2\varepsilon N_d \phi_b/q)^{1/2}$ [23] and the depletion layer width (t) of the either side at the grain boundaries was determined by the equation $N_d t = N_t$ [24].

The DC-accelerated aging stress test was performed under four continuous conditions, such as 0.85 $V_{1\,mA}$/115 °C/24 h in the first stress, 0.90 $V_{1\,mA}$/120 °C/24 h in the second stress, 0.95 $V_{1\,mA}$/125 °C/24 h in the third stress, and 0.95 $V_{1\,mA}$/150 °C/24 h in the fourth stress. Simultaneously, the leakage current was monitored at intervals of 1 min during stressing using a high voltage source-measure unit (Keithley 237). The degradation rate coefficient (K_T) was calculated from the expression $I_L = I_{Lo} + K_T t^{1/2}$ [25], where I_L is the leakage current at stress time (t) and I_{Lo} is I_L at $t = 0$. After the respective stresses, the V–I characteristics were measured at room temperature.

The dielectric characteristics, such as the apparent dielectric constant (ε_{APP}') and dissipation factor ($\tan\delta$) were measured in the range of 100 Hz to 2 MHz using a RLC meter (QuadTech 7600).

3. Results and discussion

Fig. 1 shows SEM micrographs of ZPCCD-based ceramics with various Dy_2O_3 contents. SEM micrographs clearly show the influence of Dy_2O_3 incorporation on the density and grain size. The sintered microstructure was less densified due to increasing porosity as Dy_2O_3 content increases. The increase of Dy_2O_3 content lead to the decrease of densification, as revealed in Y_2O_3-based ceramics [18]. As a result, the density of ceramics was decreased gradually in the range of 5.53–4.43 g/cm^3 corresponding to 95.7–76.6% of theoretical density (TD = 5.78 g/cm^3 in ZnO). The average ZnO grain size was saliently decreased in the range of 18.6–4.7 μm with increasing Dy_2O_3 content. The decrease of grain size is attributed to the precipitation of secondary phase in the grain boundaries and nodal points.

Fig. 2 shows the XRD patterns of ZPCCD-based ceramics with various Dy_2O_3 contents. All varistor ceramics have only two phases, i.e. ZnO grain and intergranular layer, as revealed in the former work [11,12,18]. Intergranular layer was composed of Pr_6O_{11} (or Pr_2O_3) and Dy_2O_3, and identified by EDS analysis to coexist in the grain boundaries and the nodal points. There is no so large difference in microstructure, compared with existing Pr_6O_{11}-based ZnO varistor ceramics. The detailed microstructural parameters are summarized in Table 1.

Fig. 3 shows the electric field–current density (E–J) characteristics of ZPCCD-based varistor cermics with various Dy_2O_3 contents. It can be seen that the knee region of E–J curves with Dy_2O_3 is much keener than that without Dy_2O_3 and especially, for the varistors with 0.5 mol%

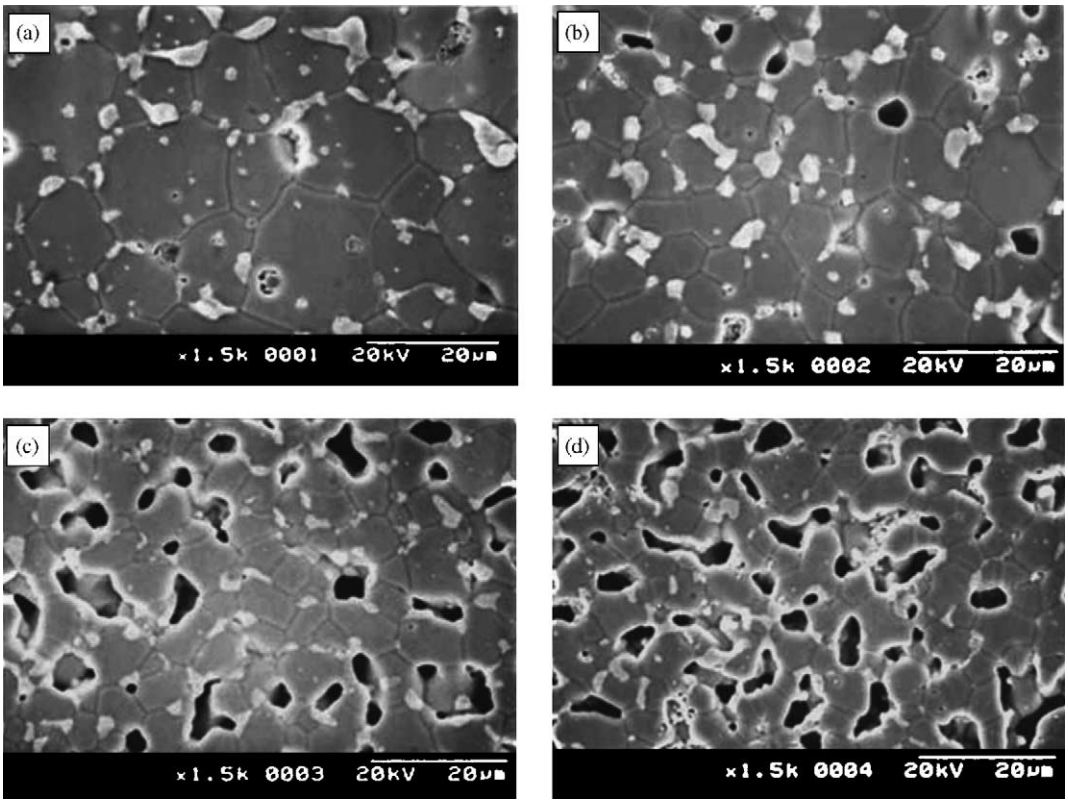

Fig. 1. SEM micrographs of ZPCCD-based ceramics with various Dy_2O_3 contents: (a) 0.0 mol%, (b) 0.5 mol%, (c) 1.0 mol%, and (d) 2.0 mol%.

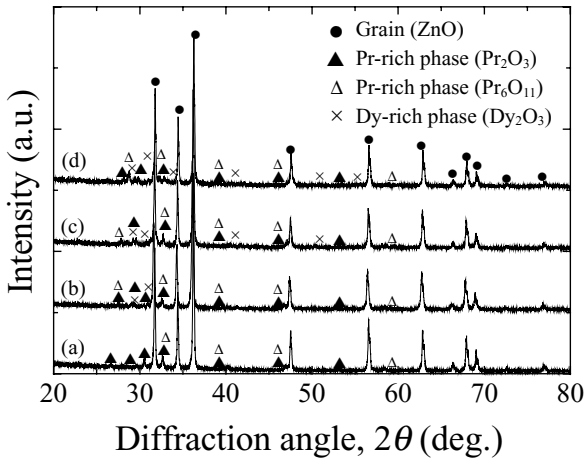

Fig. 2. XRD patterns of ZPCCD-based ceramics with various Dy_2O_3 contents: (a) 0.0 mol%, (b) 0.5 mol%, (c) 1.0 mol%, and (d) 2.0 mol%.

Table 1
The microstructural and *V–I* characteristic parameters of ZPCCD-based varistor ceramics with various Dy_2O_3 contents

Dy_2O_3 content (mol%)	d (μm)	ρ (g/cm^3)	$V_{1\,mA}$ (V/mm)	V_{gb} (V/gb)	α	I_L (μA)
0.0	18.6	5.5	39.4	0.7	4.5	87.9
0.5	11.5	5.4	223.8	2.6	66.6	1.2
1.0	6.8	4.6	345.4	2.4	34.2	3.7
2.0	4.7	4.4	436.6	2.0	37.0	2.4

Dy_2O_3. Clearly, the incorporation of Dy_2O_3 greatly improved the nonlinear properties of varistors. The varistor voltage ($V_{1\,mA}$) was greatly increased in the range of 39.4–436.6 *V*/mm. This is attributed to the increase of the number of active grain boundaries due to the decrease of ZnO grain size with increasing Dy_2O_3 content. The average breakdown voltage per grain boundaries (V_{gb}) in series between electrodes, the so-called micro-varistor voltage, is defined as following equation: $V_{gb} = (d/D)V_{1\,mA}$, where d is the average grain size and D is the thickness of sample. In other words, the larger the grain size, the lower the varistor voltage. The V_{gb} was in the range of 2.1–2.6

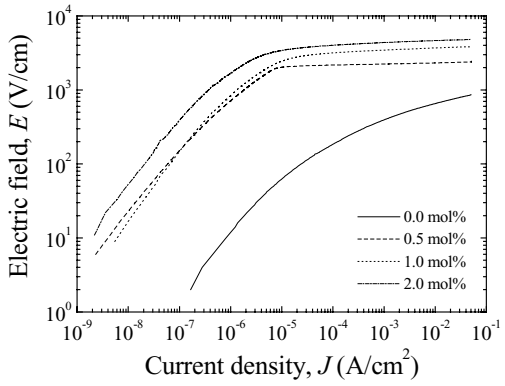

Fig. 3. The *E–J* characteristics of ZPCCD-based varistor ceramics with various Dy_2O_3 contents.

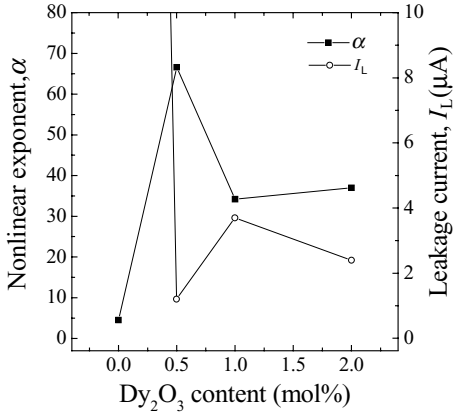

Fig. 4. The variation of nonlinear exponent and leakage current as a function of Dy_2O_3 content of ZPCCD-based varistor ceramics.

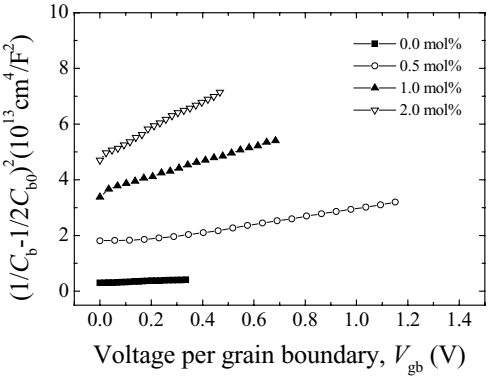

Fig. 5. The *C–V* characteristics of ZPCCD-based varistor ceramics with various Dy_2O_3 contents.

V/gb in the varistors with Dy_2O_3 and this agrees to generally well-known 2–3 *V*/gb regardless of sintering process and compositions. But the V_{gb} of varistor without Dy_2O_3 was only 0.7 *V*/gb and the ZPCC-based varistor ceramics without Dy_2O_3 is suggested to have poor grain boundaries. Generally, the varistors with V_{gb} below 1.0 *V*/gb exhibit very poor nonlinear properties. It is indicated in Fig. 4 that these grain boundaries cause very low nonlinear properties.

Fig. 4 shows the variation of nonlinear exponent (α) and leakage current (I_L) of ZPCCD-based varistor ceramics with various Dy_2O_3 contents. The α value in varistors without Dy_2O_3 was only 4.5, whereas the α value of the varistors with Dy_2O_3 was abruptly increased above 30. Then, the α value varied from maximum (66.6) in 0.5 mol% Dy_2O_3 content to minimum (34.2) in 1.0 mol% Dy_2O_3 content. The maximum α value is much higher than that for incorporation of Er_2O_3 and Y_2O_3 reported already in equivalent conditions [12–15,17,18]. The I_L value in varistor ceramics without Dy_2O_3 was 87.9 μA, whereas the I_L value of the varistor ceramics with Dy_2O_3 was very abruptly decreased below 4 μA. The minimum value of I_L was obtained from 0.5 mol% Dy_2O_3, exhibiting 1.2 μA. The variation of I_L value revealed the opposite curve to that of α value. As a result, the incorporation of Dy_2O_3 was confirmed to significantly improve the nonlinear properties. The detailed *V–I* characteristic parameters are summarized in Table 1.

The capacitance–voltage (*C–V*) characteristics of ZPCCD-based varistor ceramics with various Dy_2O_3 contents are shown in Fig. 5. It can be forecasted that Dy_2O_3 greatly affects *C–V* characteristics from the line slope and distribution. Fig. 6 shows the variation of donor concentration (N_d) and depletion layer width (t) with various Dy_2O_3 contents. The donor concentration (N_d) was decreased in the range of 4.19×10^{18} to $0.33 \times 10^{18}/cm^3$ as with increasing Dy_2O_3 content. Although Dy^{+3} ions have a larger radius (0.091 nm) than Zn^{+2} ions (0.074 nm), limited substitution within the ZnO grains is possible. Dy substitutes for Zn and creates lattice defect in ZnO grains. The chemical-defect reaction using Kroger–Vink notation can be written as

$$Dy_2O_3 \xrightarrow{ZnO} 2Dy_{Zn}^{\bullet} + V''_{Zn} + 2O_O^{\times} + 1/2O_2,$$

where $Dy_{Zn}^{\bullet}$ is a positively charged Dy ion substituted for Zn lattice site, V''_{Zn} is a negatively charged Zn vacancy, and $O_o^{\times}$ is a neutral oxygen of oxygen lattice site. The oxygen generated in reaction above affects the donor concentration. In other words, N_d is related to the partial pressure of oxygen (pO_2), namely, $N_d \propto pO_2^{-1/4}$ or $pO_2^{-1/6}$. It is, therefore, assumed that the decrease of N_d with Dy_2O_3 content is attributed to the increase of partial pressure of oxygen [10,11]. As a result, Dy_2O_3 serves as acceptor. The rare-earth oxides in Pr_6O_{11}-based varistor ceramics are found to act as an acceptor [14,18]. The increase of the depletion layer width (t) is attributed to the decrease of donor concentration. Really, the t is wider at side of lower doping region. The detailed *C–V* characteristic parameters are given in Table 2. While, with increasing Dy_2O_3 content, the density of interface states (N_t) was decreased in the range of 5.38×10^{12} to $1.74 \times 10^{12}/cm^2$. The barrier height (ϕ_b) was increased up to 1.0 mol% and thereafter decreased with increasing Dy_2O_3 content. The ϕ_b is directly connected with the N_d and N_t. In other words, the ϕ_b is estimated by the variation rate in the N_t and N_d. In general, the ϕ_b increases with

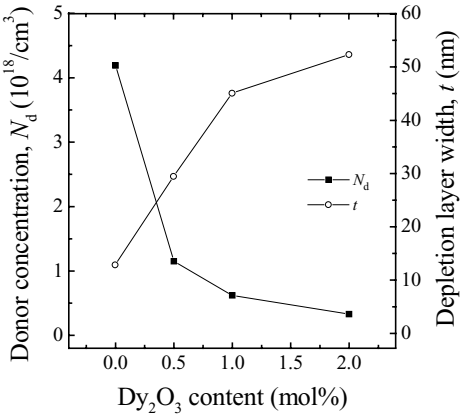

Fig. 6. The variation of donor concentration and depletion layer width as a function of Dy_2O_3 content of ZPCCD-based varistor ceramics.

Table 2
The *C–V* characteristic parameters of ZPCCD-based varistor ceramics with various Dy_2O_3 contents

Dy_2O_3 content (mol%)	N_d (10^{18} cm^{-3})	N_t (10^{12} cm^{-2})	ϕ_b (eV)	t (nm)
0.0	4.19	5.38	0.74	12.9
0.5	1.15	3.40	1.07	29.5
1.0	0.62	2.79	1.34	45.1
2.0	0.33	1.74	0.97	52.3

increasing N_t and decreasing N_d. If the variation rate of N_d is much larger than that of N_t with an additive content, the ϕ_b is much more strongly affected the N_d than the N_t. According to this reason, it can be understood that the ϕ_b is varied with increasing Dy_2O_3 content. The detailed *C–V* characteristic parameters are summarized in Table 2.

Fig. 7 shows the frequency dependence of dielectric constant (ε_{APP}') and dissipation factor ($\tan\delta$) of ZPCCD-based varistor ceramics with Dy_2O_3 content. The apparent dielectric constant (ε_{APP}') was decreased very slowly without a sharper dispersive drop evident increasing frequency, which is associated with the polarization of dielectrics. The ε_{APP}' in the measuring frequency range decreases with increasing Dy_2O_3 content. This is directly related to the average grain size, as can be seen in the following equation, $\varepsilon_{APP}' = \varepsilon_g(d/t)$, where ε_g is the dielectric constant of ZnO (8.5), d is the average grain size, and t is the depletion layer width.

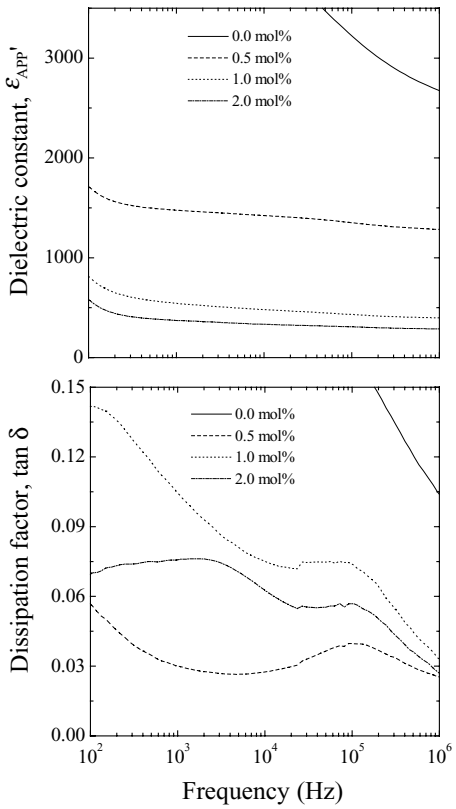

Fig. 7. Frequency variation of dielectric parameters of ZPCCD-based varistor ceramics with various Dy_2O_3 contents.

Table 3
The dielectric parameters of ZPCCD-based varistor ceramics with various Dy_2O_3 contents

Dy_2O_3 content (mol%)	0.0	0.5	1.0	2.0
ε_{APP}'	5982.3	1477.5	545.8	373.6
$\tan\delta$ (%)	34.2	3.0	10.5	7.6

That is, this is because the increase of Dy_2O_3 content causes the increase of total depletion layer width within entire bulk due to the decrease of average grain size. The detailed dielectric parameters, including the apparent dielectric constant (ε_{APP}') and dissipation factor ($\tan\delta$) are summarized in Table 3. The variation of $\tan\delta$ according to increasing frequency exhibits a complicated curve, with no remarkable dielectric absorption phenomenon except for the varistor ceramics with 0.5 mol% Dy_2O_3. In the varistor ceramics with 0.5 mol% Dy_2O_3, the $\tan\delta$ is decreased as frequency increases until a minimum. After a minimum, the $\tan\delta$ increased to maximum with increasing frequency and thereafter again decreased. This is typical curve of $\tan\delta$ in the varistors. It was found that the values of $\tan\delta$ are greatly affected by various Dy_2O_3 contents. The $\tan\delta$ was increased in the range of $\tan\delta = 0.030$–0.342 with increasing Dy_2O_3 contents at 1 kHz and was the lowest as 0.030 in the varistor ceramics with 0.5 mol% Dy_2O_3. The $\tan\delta$ variation of all varistor ceramics showed the same tendency as variation of leakage current. The detailed dielectric parameters are summarized in Table 3.

In application of varistors, two important factors that should be necessarily considered are the nonlinearity of *V–I* properties and its stability. The electronic and electrical systems to be protected from various surges significantly require a high stability of varistor ceramics itself above all in order to enhance their reliability. In practice, ZnO varistor ceramics begin to degrade because of gradually increasing leakage current with stress time. Eventually, they loss a varistor function due to the thermal runaway. Therefore, the electrical stability of the varistor is far more important than other things. In this viewpoint, in addition to nonlinearity, the electrical stability is technologically very important characteristic of ZnO varistor ceramics. The electrical stability can be estimated by AC and impulse, etc. in addition to DC, as tried in this paper.

Fig. 8 shows the leakage current during various DC-accelerated aging stresses of ZPCCD-based varistor ceramics with various Dy_2O_3 contents. The varistors with Dy_2O_3 of 1.0 and 2.0 mol% exhibited the thermal runaway within a short time, even under the first stress (0.85 $V_{1\,mA}$/115 °C/24 h). The varistors stressed were completely degraded. This poor stability may be attributed to the low density, which decreases the number of conduction path and eventually leads to the concentration of current. The leakage current of these varistors is low, but the density is very low below 80% TD. The stability against DC-accelerated aging stress seems to be affected more predominantly by density

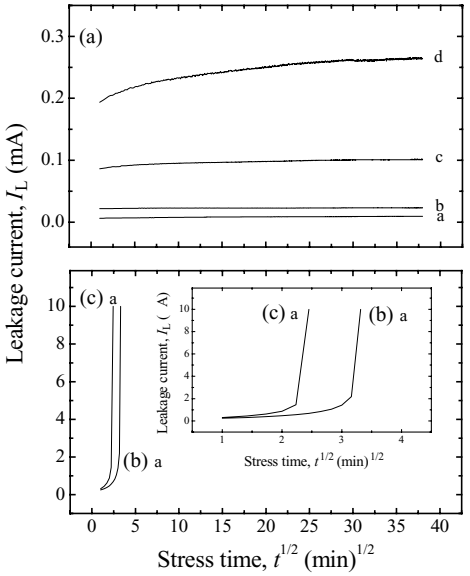

Fig. 8. The leakage current during various DC-accelerated aging stresses of ZPCCD-based varistor ceramics with various Dy_2O_3 contents: (a) 0.5 mol%, (b) 1.0 mol%, (c) 2.0 mol%; a: the first stress, b: the second stress, c: the third stress, and d: the fourth stress.

than leakage current. On the contrary, the varistors with 0.5 mol% Dy_2O_3 exhibited far better stability, compared with the varistors with 1.0 and 2.0 mol% Dy_2O_3. Its leakage current exhibited nearly constant value until the second stress (0.90 $V_{1\,mA}$/120 °C/24 h), but weak positive creep of leakage current (PCLC) during the third stress and remarkable creep during the fourth stress (0.95 $V_{1\,mA}$/150 °C/24 h). The stability of varistors can be estimated by the degradation rate coefficient (K_T), indicating the degree of aging. The lower the K_T, the higher the stability. The K_T of varistor with 0.5 mol% Dy_2O_3 was 0.39 μA $h^{-1/2}$ after the first stress, however, that was lowered in 0.21 μA $h^{-1/2}$ rather after the second stress (0.90 $V_{1\,mA}$/120 °C/24 h). It is suggested that this is attributed to stabilization of grain boundaries due to DC-accelerated aging stress, like both electrical and thermal stimulation. After further stress, the K_T greatly increased up to 1.66 μA $h^{-1/2}$ in the third stress (0.95 $V_{1\,mA}$/125 °C/24 h) and abruptly increased up to 7.82 μA $h^{-1/2}$ in the fourth stress (0.95 $V_{1\,mA}$/150 °C/24 h). To exhibit good stability in the varistor ceramics with 0.5 mol% Dy_2O_3, compared with other varistor ceramics, is attributed to high density and low leakage cuurent.

Fig. 9 shows the variation of *E–J* curve of ZPCCD-based varistor ceramics with various DC-accelerated aging stress. It can be seen that on the whole, the curve is greatly varied in the prebreakdown region, compared with breakdown region after DC-accelerated aging stress. Since the degradation results from ultimately leakage current due to the thermionic emission, the curve in the prebreakdown region, called leakage current region, is largely changed. With proceeding degradation, the curves in the prebreakdown region shift toward low electric field and high current density.

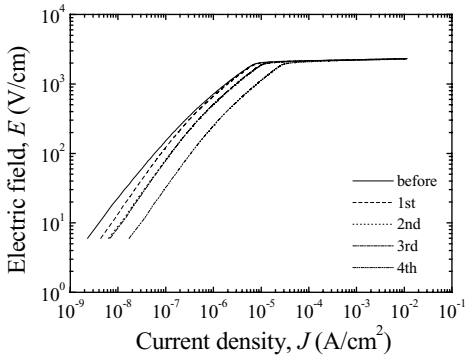

Fig. 9. The *E–J* characteristics of ZPCCD-based varistor with 0.5 mol% Dy_2O_3 before and after DC-accelerated aging stress.

Fig. 10 shows the variation rate of the varistor voltage (%$\Delta V_{1\,mA}$), variation rate of the nonlinear exponent (%$\Delta\alpha$), and variation rate of the leakage current (%ΔI_L) after various DC-accelerated aging stresses, for the varistors with 0.5 mol% Dy_2O_3, with no thermal runaway even under the fourth stress (0.95 $V_{1\,mA}$/150 °C/24 h). In an aspect of the stability of *V–I* characteristics, the %$\Delta V_{1\,mA}$ should be lower than other variation rate of parameters. In general, the allowed specifications of %$\Delta V_{1\,mA}$ for the commercial varistors are less than 10% under 0.85 $V_{1\,mA}$/85 °C/1000 h. Even though the stressing time in this study is short, the stressing voltage and ambient temperature are very severe. On the whole, the varistor voltage exhibited comparatively much lower variation rate than those of other parameters with DC stress strength. This varistor exhibited a high stability by marking %$\Delta V_{1\,mA} = -1.9\%$, %$\Delta\alpha = -10.5\%$, and %$\Delta I_L = +288.8\%$ after the fourth stress (0.95 $V_{1\,mA}$/150 °C/24 h). Then this varistor still exhibited good nonlinear properties, in which the nonlinear exponent is 59.6 and the leakage current is 4.5 μA.

Fig. 11 shows the variation of dielectric parameters, such as the variation rate of dielectric constant (%$\Delta\varepsilon_{APP}'$) and the variation rate of dissipation factor (%$\Delta\tan\delta$) after various DC-accelerated aging stresses, for the varistor ceramics with

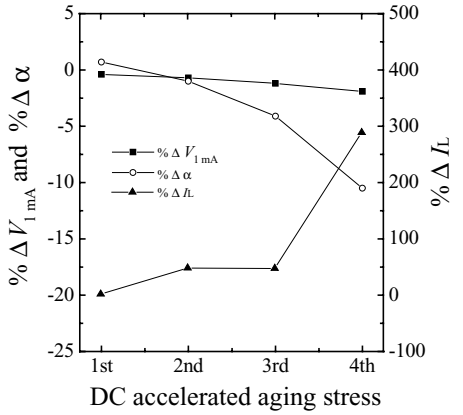

Fig. 10. The variation rate of *V–I* characteristic parameters of ZPCCD-based varistor ceramics with 0.5 mol% Dy_2O_3.

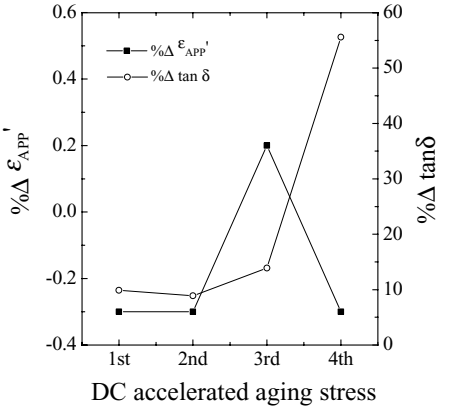

Fig. 11. The variation rate of dielectric characteristic parameters of ZPCCD-based varistor ceramics with 0.5 mol% Dy_2O_3.

0.5 mol% Dy_2O_3. The ε_{APP}' hardly changed in the range of ±0.3% through entire stress, and the $\tan\delta$ did not change so greatly as $\%\Delta\tan\delta = +13.9\%$ until the third stress, whereas it changed more and less as $\%\Delta\tan\delta = +55.6\%$ after the fourth stress. Then this varistor still exhibited low $\tan\delta$, 0.047.

4. Conclusions

The microstructure, electrical characteristics, and their stability for DC-accelerated aging stress of ZPCCD ($ZnO–Pr_6O_{11}–CoO–Cr_2O_3–Dy_2O_3$)-based varistor ceramics were investigated at various Dy_2O_3 contents. ZPCCD-based ceramics revealed a simple microstructure composing of ZnO grain and intergranular layer. The density of ZPCCD-based ceramics was decreased with increasing Dy_2O_3 content. The nonlinear properties were greatly enhanced by incorporation of Dy_2O_3. The varistor with Dy_2O_3 of 0.5 mol% exhibited a good nonlinearity, with the nonlinear exponent of 66.6 and the leakage current of 1.2 μA, compared with the varistors without Dy_2O_3, in which the nonlinear exponent is 4.5 and the leakage current is 87.9 μA. In addition, this varistor exhibited low dissipation factor of 0.030.

Furthermore, this varistor exhibited relatively good stability as marking $\%\Delta V_{1\,mA} = -1.9\%$, $\%\Delta\alpha = -10.5\%$, $\%\Delta I_L = +288.8\%$, and $\%\Delta\tan\delta = +55.6\%$ in DC-accelerated aging stress (0.95 $V_{1\,mA}$/150 °C/24 h). This varistor still good electrical properties with 59.6 in nonlinear exponent, 4.5 μA in leakage current, and 0.047 in dissipation factor. Therefore, it is forecasted that this varistor will be sufficiently applied to surge absorbers.

Acknowledgements

This work was supported by EEC (Electronic Ceramics Center) at Dongeui University as RRC·TIC program through KOSEF (Korea Science and Engineering Foundation), ITEP (Korea Institute of Industrial Technology Evaluation and Planning), and Busan Metropolitan City.

References

[1] L.M. Levinson, H.R. Pilipp, Zinc oxide varistor—a review, Am. Ceram. Soc. Bull. 65 (1986) 639–646.
[2] T.K. Gupta, Application of zinc oxide varistor, J. Am. Ceram. Soc. 73 (1990) 1817–1840.
[3] Y.-S. Lee, T.-Y. Tseng, Phase identification and electrical properties in ZnO–glass varistors, J. Am. Ceram. Soc. 75 (1992) 1636–1640.
[4] A.B. Alles, V.L. Burdick, The effect of liquid-phase sintering on the properties of Pr_6O_{11}-based ZnO varistors, J. Appl. Phys. 70 (1991) 6883–6890.
[5] A.B. Alles, R. Puskas, G. Callahan, V.L. Burdick, Compositional effect on the liquid-phase sintering of praseodymium oxides-based ZnO varistors, J. Am. Ceram. Soc. 76 (1993) 2098–2102.
[6] Y.-S. Lee, K.-S. Liao, T.-Y. Tseng, Microstructure and crystal phases of praseodymium in zinc oxides varistor ceramics, J. Am. Ceram. Soc. 79 (1996) 2379–2384.
[7] N. Wakiya, S.Y. Chun, C.H. Lee, O. Sakurai, K. Shinozaki, N. Mizutani, Effect of liquid phase and vaporization on the formation of microstructure of Pr doped ZnO varistor, J. Electroceram. 4 (S1) (1999) 15–23.
[8] S.Y. Chun, K. Shinozaki, N. Mizutani, Formation of varistor characteristics by the grain-boundaries penetration of $ZnO–PrO_x$ liquid into ZnO ceramics, J. Am. Ceram. Soc. 82 (1999) 3065–3068.
[9] S.Y. Chun, N. Mizutani, Mass transport via grain boundary in Pr-based ZnO varistors and related electrical effects, Mater. Sci. Eng. B79 (2001) 1–5.
[10] C.-W. Nahm, The electrical properties and d.c. degradation characteristics of Dy_2O_3 doped Pr_6O_{11}-based ZnO varistors, J. Eur. Ceram. Soc. 21 (2001) 545–553.
[11] C.-W. Nahm, C.-H. Park, Effect of Er_2O_3 addition on the microstructure, electrical properties, and stability of Pr_6O_{11}-based ZnO ceramic varistors, J. Mater. Sci. 36 (2001) 1671–1677.
[12] C.-W. Nahm, The nonlinear properties and stability of $ZnO–Pr_6O_{11}–CoO–Cr_2O_3–Er_2O_3$ ceramic varistors, Mater. Lett. 47 (2001) 182–187.
[13] C.-W. Nahm, H.-S. Yoon, J.-S. Ryu, The nonlinear properties and d.c. degradation characteristics of ZPCCE based varistors, J. Mater. Sci. Lett. 20 (2001) 393–395.
[14] C.-W. Nahm, B.-C. Shin, Effect of sintering temperature on electrical properties and stability of Pr_6O_{11}-based ZnO varistors, J. Mater. Sci.: Mater. Electron. 13 (2002) 111–120.
[15] C.-W. Nahm, $ZnO–Pr_6O_{11}–CoO–Cr_2O_3–Er_2O_3$-based ceramic varistors with high stability of nonlinear properties, J. Mater. Sci. Lett. 21 (2002) 201–204.
[16] C.-W. Nahm, J.-S. Ryu, Influence of sintering temperature on varistor characteristics of ZPCCE-based ceramics, Mater. Lett. 53 (2002) 110–116.
[17] C.-W. Nahm, H.-S. Kim, Effect of Pr_6O_{11}/CoO mole ratio on nonlinear properties and DC accelerated aging characteristics of $ZnO–Pr_6O_{11}–CoO–Dy_2O_3$ based varistors, Mater. Lett. 56 (2002) 379–385.
[18] C.-W. Nahm, Microstructure and electrical properties of Y_2O_3 doped $ZnO–Pr_6O_{11}$-based varistor, Mater. Lett. 57 (2003) 1317–1321.
[19] C.-W. Nahm, B.-C. Shin, Highly stable electrical properties of $ZnO–Pr_6O_{11}–CoO–Cr_2O_3–Y_2O_3$-based varistor cearmics, Mater. Lett. 57 (2003) 1322–1326.
[20] C.-W. Nahm, H.-S. Kim, Influence of cooling rate on stability of nonlinear properties of $ZnO–Pr_6O_{11}$-based varistor ceramics, Mater. Lett. 57 (2003) 1544–1549.

[21] C.-W. Nahm, Nonlinear properties and stability against DC accelerated aging of praseodymium oxide-based ZnO varistors by Er_2O_3 doping, Solid State Commun. 126 (2003) 281–284.
[22] J.C. Wurst, J.A. Nelson, Lineal intercept technique for measuring grain size in two-phase polycrystalline ceramics, J. Am. Ceram. Soc. 55 (1972) 109–111.
[23] M. Mukae, K. Tsuda, I. Nagasawa, Capacitance-vs-voltage characteristics of ZnO varistor, J. Appl. Phys. 50 (1979) 4475–4476.
[24] L. Hozer, Semiconductor Ceramics: Grain Boundary Effects, Ellis Horwood, London, 1999, p. 22.
[25] J. Fan, R. Freer, Deep level transient spectroscopy of zinc oxide varistors doped with aluminum oxide and/or silver oxide, J. Am. Ceram. Soc. 77 (1994) 2663–2668.